


# A novel WT1 gene mutation in a chinese girl with denys-drash syndrome

Faliang Wang<sup>1</sup>  | Jiabin Cai<sup>1</sup> | Jinhua Wang<sup>1</sup> | Min He<sup>1</sup> | Junqing Mao<sup>1</sup> | Kun Zhu<sup>2</sup> | Manli Zhao<sup>2</sup> | Zhonghai Guan<sup>1</sup> | Linjie Li<sup>1</sup> | Hongchuan Jin<sup>3</sup> | Qiang Shu<sup>1</sup>

<sup>1</sup>Department of Surgical Oncology, Children's Hospital, National Clinical Research Center for Child Health, Zhejiang University School of Medicine, Hangzhou, China

<sup>2</sup>Department of Pathology, Children's Hospital, National Clinical Research Center for Child Health, Zhejiang University School of Medicine, Hangzhou, China

<sup>3</sup>Laboratory of Cancer Biology, Key Lab of Biotherapy in Zhejiang, Sir Run Run Shaw Hospital, Zhejiang University School of Medicine, Hangzhou, China

## Correspondence

Faliang Wang and Qiang Shu, Department of Surgical Oncology, Children's Hospital, National Clinical Research Center for Child Health, Zhejiang University School of Medicine, Hangzhou, Zhejiang, China. Emails: 21118179@zju.edu.cn (FW); shuqiang@zju.edu.cn (QS)

## Funding information

National Natural Foundation of China, Grant/Award Number: 81801939; Health Commission of Zhejiang Province, Grant/Award Number: 2019KY093

## Abstract

**Objective:** Denys-Drash syndrome (DDS) is defined by the triad of Wilms tumor, nephrotic syndrome, and/or ambiguous genitalia. Genetic testing may help identify new gene mutation sites and play an important role in clinical decision-making.

**Methods:** We present a patient with an XY karyotype and female appearance, nephropathy, and Wilms tumor in the right kidney. Genomic DNA was extracted from peripheral blood cells according to standard protocols. "Next-generation" sequencing (NGS) was performed to identify novel variants. The variant was analyzed with Mutation Taster, and its function was explored by a cell growth inhibition assay.

**Results:** We found the first case of Denys-Drash syndrome with the uncommon missense mutation (c.1420C>T, p.His474 Tyr) in the WT1 gene. In silico analysis, the variant was predicted "disease-causing" by Mutation Taster. The mutated variant showed a weaker effect in inhibiting tumor cells than wild-type WT1.

**Conclusions:** The uncommon missense mutation (c.1420C>T, p.His474 Tyr) in the WT1 gene may be a crucial marker in DDS.

## KEYWORDS

46, Denys-Drash syndrome (DDS), nephrotic syndrome, Wilms tumor, Wilms tumor-1 (WT1), XY karyotype

## 1 | INTRODUCTION

DDS is a rare genetic disorder of sex development featuring a triad of Wilms' tumor, nephrotic syndrome, and the 46, XY karyotype. DDS is correlated with heterozygous missense mutations in the zinc-finger (ZF) region of the WT1 gene, which is a tumor suppressor gene involved in gonadal development and is located in chromosome band 11p13.<sup>1,2</sup>

The WT1 gene encodes a zinc-finger transcription factor that is important for the normal development of the genital tract and the kidneys.<sup>3</sup> Genitourinary defects were found in WT1 knockout mice

that died on embryonic day 13.5.<sup>4</sup> The WT1 gene comprises ten coding exons. The first six exons encode a glutamine- and proline-rich N-terminal region containing a potential RNA recognition motif, involved in self-association, localization to nuclear speckles, transcriptional activation and repression, and nuclear export. The last four exons are also crucial for the function of WT1. They encode a ZF domain that plays a key role in DNA/RNA binding and nuclear localization.<sup>5,6</sup> Mutations in exons 8 or 9 are very common in DDS patients.<sup>7</sup>

In this study, we present a patient with Wilms tumor, a female appearance, and a 46, XY karyotype who had previously unreported mutations in exon 9 in the ZF3 region of WT1 (Figure 1).

This is an open access article under the terms of the Creative Commons Attribution License, which permits use, distribution and reproduction in any medium, provided the original work is properly cited.

© 2021 The Authors. *Journal of Clinical Laboratory Analysis* published by Wiley Periodicals LLC

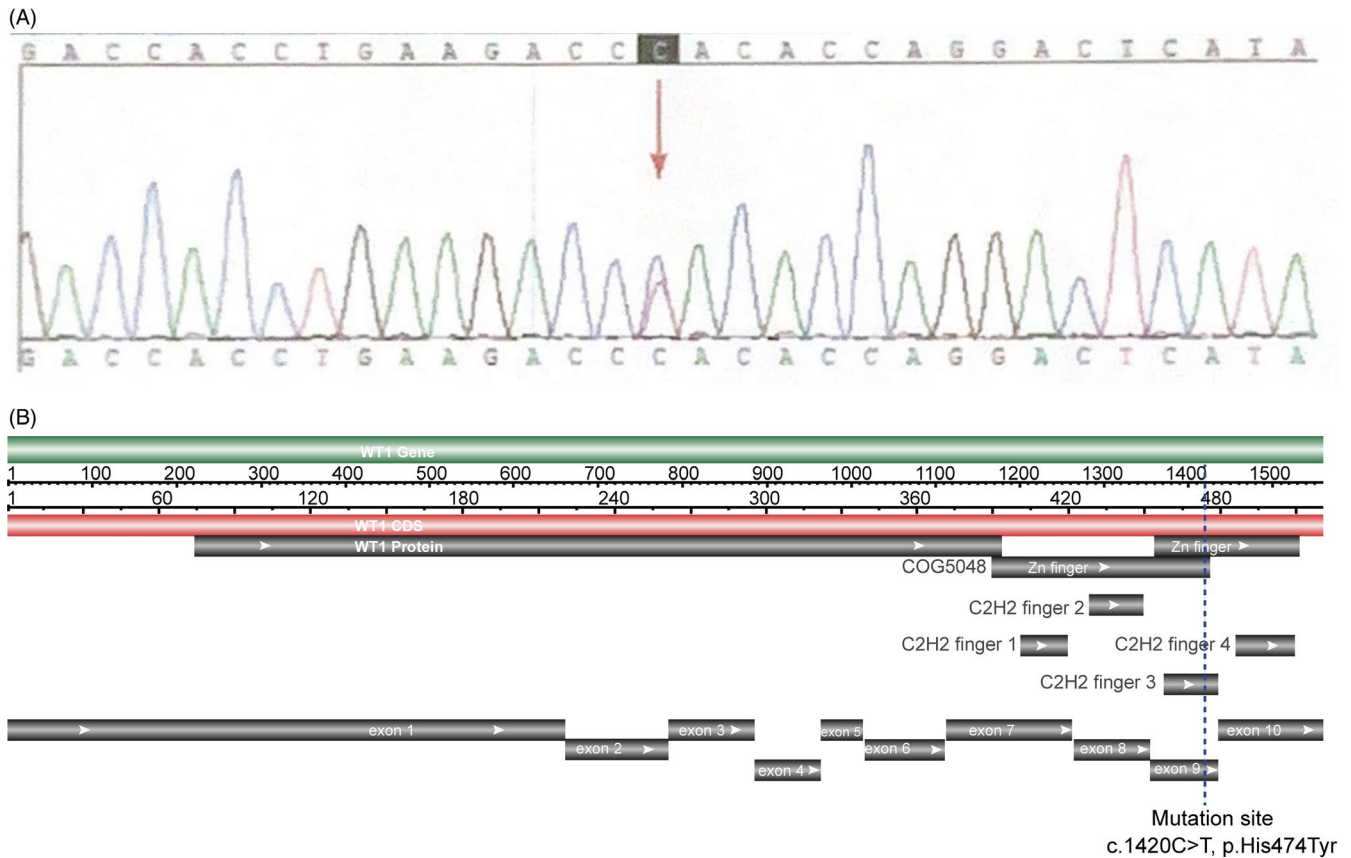


**FIGURE 1** A, Sanger sequencing chromatogram shows the double peak C/T in WT1 gene. B, The location of the mutation site detected in the Coding DNA Sequence (CDS) of WT1. The NCBI Reference number is NM\_024424.5

## 2 | METHODS

### 2.1 | Participants

A 23-month-old girl with DDS and her parents from Zhejiang Province were enrolled in this study at the Department of Surgical Oncology, Children's Hospital, Zhejiang University School of Medicine, Hangzhou, Zhejiang, China (Figure 2). The study was approved by the ethics committee of Children's Hospital, Zhejiang University School of Medicine, Hangzhou, China, and the participants and guardians provided written informed consent in accordance with the recommendations of the Declaration of Helsinki.

### 2.2 | Clinical assessment

A comprehensive clinical examination of the abdominal mass was performed. We conducted an ordinary physical examination, laboratory tests [routine blood, urine and fecal, liver and kidney function, electrolyte, tumor makers, and sex-determining region on the Y chromosome (SRY)], and imageological examinations [electrocardiogram, abdominal B-ultrasonography examination, and contrast-enhanced computed tomography (CT)]. After that, a puncture biopsy was performed.

### 2.3 | Clinical treatment

Based on the diagnosis of nephroblastoma (mesenchymal type), the patient was treated with chemotherapy, arterial interventional therapy, and nephroblastoma radical resection. Detailed information is summarized in Table 1.

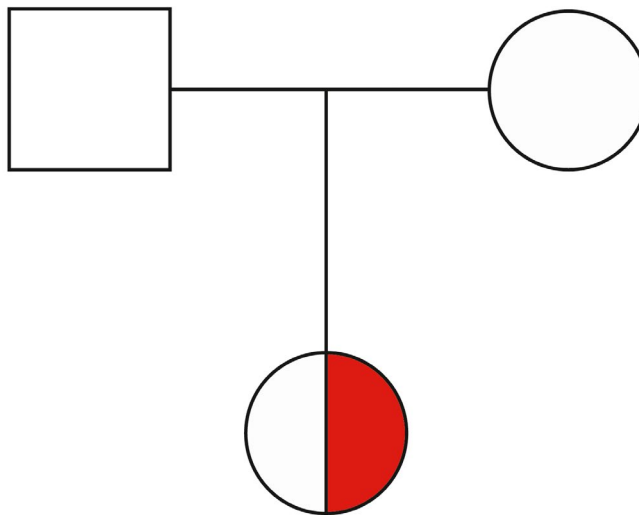
### 2.4 | Genetic testing

The identification process is a two-step procedure: High-throughput sequencing technologies and validation of suspected disease-causing mutations (Sanger sequencing).

#### 2.4.1 | High-throughput sequencing

To make a precise diagnosis, we performed targeted "Next-generation" sequencing (NGS) of 175 disease-related genes. Written informed consent of the whole family was obtained prior to the collection of 5 mL of their peripheral blood for the following experiment. The study was approved by the ethics committee of the Beijing Genomics Institute (BGI).

**FIGURE 2** A pedigree diagram illustrating the heterozygous missense mutation in *WT1* gene in the patient's family. The half-filled symbol indicates the proband (heterozygous carrier)



### Patient with Denys-Drash syndrome and 46, XY karyotype

**TABLE 1** Summary of the treatment course of the patient

Time	Treatment
2015.09.29	Embolization and chemotherapy via the right femoral artery (Cisplatin +Pirarubicin + Vinorelbine)
2019.11.05	Vinorelbine +Ifosfamide + Etoposide
2015.11.20	Laparotomy, right nephroblastoma resection, lymphadenectomy, and partial adrenalectomy
2015.11.30	Vinorelbine +Pirarubicin + Carboplatin
2015.12.29	Vinorelbine +Ifosfamide + Etoposide
2016.01.22	Vinorelbine +Pirarubicin + Carboplatin
2016.03.03	Vinorelbine +Actinomycin D
2016.03.29	Vinorelbine +Carboplatin + Pirarubicin
2016.4.28	Vinorelbine +Actinomycin
2016.5.25	Vinorelbine +Pirarubicin
2016.6.23	Vinorelbine +Actinomycin D
2016.07.23	Vinorelbine +Pirarubicin

A capture panel (NimbleGen, Madison, USA) of disease-related genes was previously designed and assessed by our group. The capture panel comprised 2,433,298 bp that covered all exons together with the flanking exon and intron boundaries ( $\pm 15$  bp) of 175 disease-related genes.

Genomic DNA was extracted from peripheral blood mononuclear cells using the QIAamp DNA Blood Midi Kit (Qiagen, Hilden, Germany) according to the manufacturer's instructions. Genomic DNA was fragmented by Covaris LE220 (Massachusetts, USA). DNA fragments were ligated to platform-specific adaptors to generate DNA library (200–250 bp). The library was enriched by array hybridization according to previously published procedure,<sup>8</sup> followed by elution and post-capture amplification. The products were then subjected to Agilent 2100 Bioanalyzer and ABI StepOne to estimate the magnitude of enrichment. After quality control, captured library sequencing was

carried out on Illumina HiSeq2500 Analyzers (Illumina, San Diego, USA). Following the manufacturer's standard sequencing protocols for 90 cycles per read to generate paired-end reads. Image analysis, error estimation, and base calling were performed using Illumina Pipeline software (version 1.3.4) to generate raw data.

As for quality control, the data were processed as follows: a. Discard paired reads if either one read contains adapter contamination ( $>10$  nucleotides aligned to the adapter, allowing  $\leq 10\%$  mismatches); b. Discard paired reads if more than 10% of bases are uncertain in either read; c. Discard paired reads if the proportion of low-quality bases (Phred quality  $< 5$ ) is over 50% in either read. All downstream bioinformatics analyses were based on high-quality clean data.

The sequencing reads were aligned to the reference human genome (UCSC hg19) using BWA (Burrows-Wheeler Aligner)

Multi-Vision software package.<sup>9</sup> After alignment, the output files were used to perform sequencing coverage and depth analysis of the target region, single-nucleotide variants (SNVs), and INDEL calling. We used SOAPsn software<sup>10</sup> and Samtools<sup>11</sup> to detect SNVs and indels. All SNVs and indels were filtered and estimated via multiple databases, including NCBI dbSNP, HapMap, 1000 human genome dataset, and database of 100 Chinese healthy adults.<sup>12</sup> Pathogenic variants were assessed under the protocol issued by the American College of Medical Genetics and Genomics (ACMG).<sup>13</sup> The Human Gene Mutation Database (HGMD) was used to screen mutations reported in published studies.

## 2.4.2 | Verification of the variant

All mutations and potential pathogenic variants were validated by Sanger sequencing on an ABI3730 sequencer. The reference sequence of the WT1 gene is NM\_024424.5.

## 2.5 | In silico analysis

The mutation site was analyzed using Mutation Taster (<http://www.mutationtaster.org/>).<sup>14-16</sup>

## 2.6 | Functional analysis of the novel variant

To detect the function of the novel WT1 variant, we cloned the wild type and mutated coding DNA sequence (CDS) (NP\_077742.3) of the WT1 gene to pcDNA3.1 and compared their function by a cell growth inhibition assay.

### 2.6.1 | Plasmid construction

Total RNA was extracted from the tumor tissue using TRIzol® Reagent (Thermo Fisher Scientific). We used a QuantiTect reverse transcription kit (Qiagen) to synthesize cDNA. The full-length CDS of the WT1 gene was obtained by PCR with cDNA. The PCR primers were as follows: F-5'-GCGGATCCCTGGACTTCTTCTTGCTG-3', R-5'-GCGAATTCTCAAAGCGCCAGCTGGAG-3'. To facilitate cloning, the PCR product and the vector (pcDNA3.1) were digested by BamHI and EcoRI. The PCR product was then inserted into pcDNA3.1. The pcDNA3.1-WT1 (C1420 T) was verified by Sanger sequencing. We analyzed the nucleotide sequences according to the NCBI Reference Sequence: NM\_024424.5. The pcDNA3.1-WT1 (wild type) was generated by PCR-based site-directed mutagenesis. The primers used were as follows: F-5'-GACCACCTGAAGACCCACACCAGGACTCATA-3', R-5'-TATGAGTCCTGGTGTGGGTCTTCAGGTGGTC-3'.

### 2.6.2 | Cell culture

G401 cells were used in this study. The cell line was purchased from the Cell Bank of the Chinese Academy of Sciences (Shanghai, China). The cells were grown in DMEM supplemented with 10% FBS and 1/1000 gentamycin.

### 2.6.3 | Cell transfection

Cell transfection was performed according to the protocol of Lipofectamine 2000 (Invitrogen; Thermo Fisher Scientific, Inc.) when cells reached 60% confluence. The cells were transfected with pcDNA3.1-WT1 (wild type), pcDNA3.1-WT1 (C1420 T), and the empty vector pcDNA3.1. The ratio of Lipofectamine 2000 to plasmid was 3:1. The transfected cells were digested with trypsin and seeded in 6-well plates for western blotting, and 96-well plate for cell growth inhibition assay.

### 2.6.4 | Western blot

After the transfected cells grew for 48 h in the 6-well plate, we washed the cells with 1X PBS three times and lysed them with 100ul 1X RIPA per well. Thereafter, the protein concentration was quantified and 20 µg of proteins from each sample were segregated using 10% SDS-PAGE gel. The samples were then transferred to PVDF membranes and incubated with primary antibodies (WT1: sc-7385, Santa Cruz, 1:1000 dilution; GAPDH: sc-47724, Santa Cruz, 1:1000 dilution) and secondary antibodies (m-IgGκ BP-HRP: sc-516102, Santa Cruz, 1:2000 dilution). Finally, blots were detected with Chemiluminescent HRP Substrate reagent (Merck Millipore, Darmstadt, Germany), and the signal was captured by Bio-Rad ChemiDoc XRS+ (BioRad Laboratories, Inc., Hercules, CA, USA).

### 2.6.5 | Cell growth inhibition assay

The cell growth inhibition assay was performed using the MTS method. We seeded 3000 transfected G401 cells from each group in 96-well plates per well and cultured them for 7 days. Cell viability was tested using the MTS Cell Proliferation Assay kit (Promega) according to the standard protocol.

## 2.7 | Statistical Analysis

Statistical analysis was performed using GraphPad Prism 8.0 (GraphPad, Inc.). The data are expressed as the mean ± standard deviation. Unpaired Student's t-test was performed to evaluate

differences between groups.  $p < 0.05$  was considered to indicate a statistically significant difference. The experimental values are the means of triplicated independent repeats.

### 3 | RESULTS

#### 3.1 | Clinical findings and post-treatment follow-up

##### 3.1.1 | Physical examination

Physical examination revealed a palpable right abdominal mass with smooth margins. She also had elevated blood pressure (135/90 mmHg) and clitoral hypertrophy.

##### 3.1.2 | Imageological examinations

Abdominal contrast-enhanced CT revealed an approximately  $7.1 \times 8.0 \times 7.6$  cm heterogeneous enhancing mass in the upper region of the right kidney (Figure 3). Ultrasound imaging revealed that the

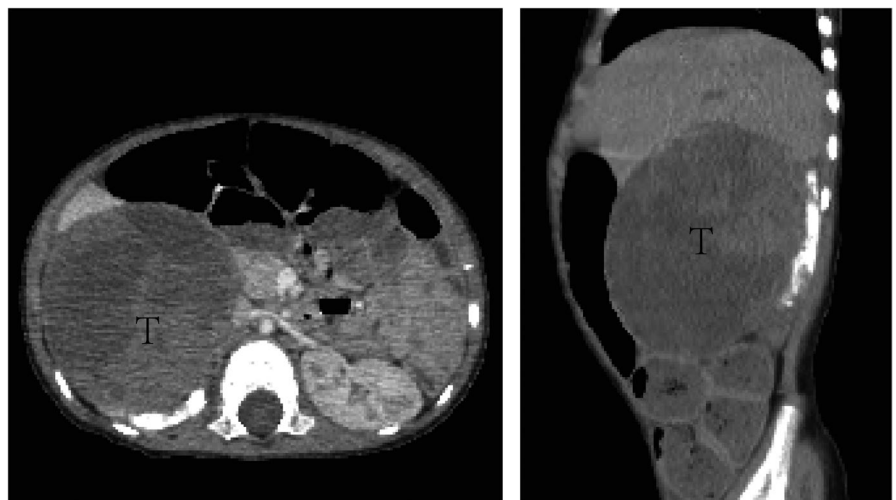
vagina, uterus, and right ovary were almost normal. However, the left ovary was not clearly delineated.

##### 3.1.3 | Laboratory tests and laparoscopic examination

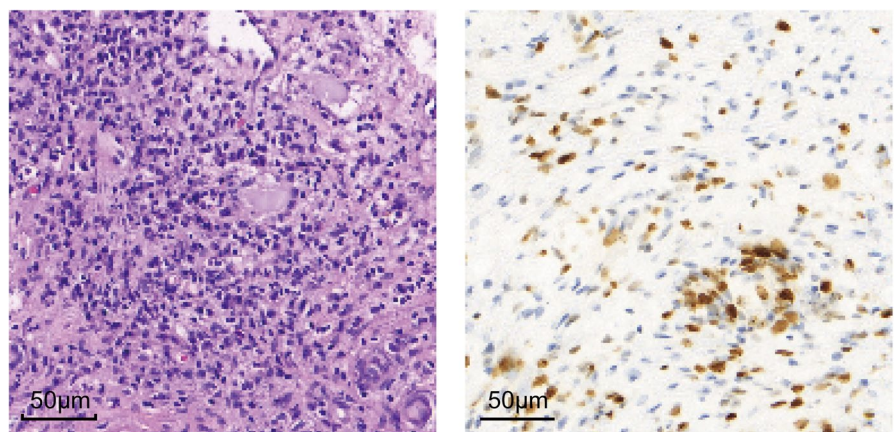
The patient had proteinuria without microscopic hematuria. She underwent a renal biopsy and histopathological examination indicated a diagnosis of Wilms tumor, and then, a right nephrectomy was performed. The pathologic report revealed a nephroblastoma (mesenchymal type) with necrosis based on the National Wilms Tumor Study Group 5 (NWTS-5) classification criteria (Figure 4). The normal renal tissue structure was clear and demonstrated no evidence of glomerulosclerosis.

After completing chemotherapy and arterial interventional therapy, we evaluated the clitoral hypertrophy. The patient's vaginal and urethral orifices were grossly normal. However, her karyotype was 46, XY. Luteinizing hormone (LH) (1.8 IU/L; normal range 1.0–4.0 IU/L) was at a normal basal level, but follicle-stimulating hormone (FSH) (128 IU/L; normal range 1.0–5.0 IU/L) was much higher than

**FIGURE 3** Contrast-enhanced CT showing the  $7.1 \text{ cm} \times 8.0 \text{ cm} \times 7.6 \text{ cm}$  sized heterogeneous enhancing mass in the upper region of the right kidney. Left: transverse view of the tumor, Right: sagittal view of the tumor



**FIGURE 4** HE staining (left) and immunohistochemical staining (WT1) (right) after tumor resection





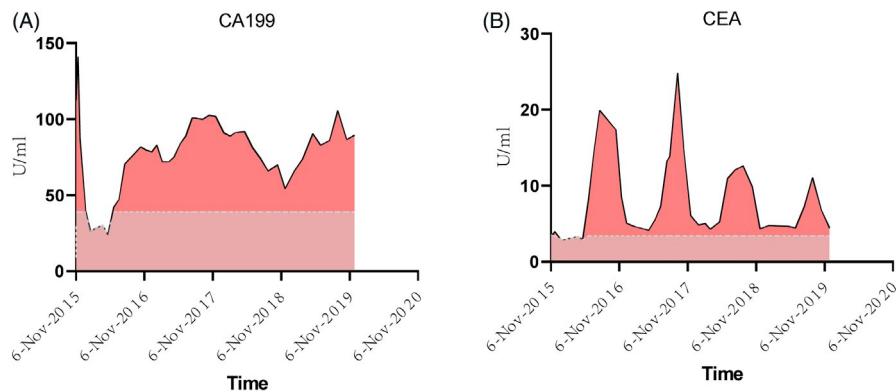


**FIGURE 5** CA199, A, and CEA B, levels in peripheral blood in the follow-up period. The full curve represents the measured value, and the dotted line represents the reference range. The last chemotherapy was on July 23, 2016

the normal basal level. Testosterone ( $< 0.01$  ng/mL; normal range 0.07–0.52 ng/mL) was very low, and no elevation was observed after hCG stimulation.

To determine whether the gonads were normal, laparoscopy was performed when the patient was 29 months old. A small uterus and fallopian tube were observed during the laparoscopic examination. In addition, both gonads were located at the lateral side of the fallopian tube, so they were partly resected for biopsies. The pathology showed that both gonads were dysgenetic testicular tissue.

### 3.1.4 | Final Diagnosis and post-treatment follow-up

All clinical manifestations and molecular analyses demonstrated that the patient had Denys-Drash syndrome. After 46 months of follow-up, the patient was in good condition and showed no signs of tumor recurrence. However, the severity of the nephropathy increased and decreased. Albumin levels (1,030–3,226 mg/L; normal children  $< 100$  mg/L) were much higher than normal levels in the first two months, but her microalbuminuria was controlled well thereafter. Blood pressure was controlled using enalapril maleate and valsartan. In addition, CEA (2.89–24.85 U/ml; normal children  $< 3.4$  U/ml) and CA199 (3.31–141 U/ml; normal children  $< 39$  U/ml) were always higher than normal in the follow-up period (Figure 5).

### 3.2 | Identification of the novel mutation

Whole exon sequencing revealed that the *WT1* mutation was positive. The patient was found to have a heterozygous missense mutation, converting 474 His to 474 Tyr (c.1420C>T, Figure 1) in exon 9 of *WT1*, encoding a portion of the *WT1* zinc-finger 3 domain.

### 3.3 | In silico analysis

The mutant variant of *WT1* (c.1420C>T, p. His474 Tyr) was predicted to “disease-causing” by Mutation Taster. The peptide alignment revealed that the histidine in *WT1* was a conserved residue (Figure 6).

Patient	KTCQRKFSRSDHLKTYTRHTG
Human	-----h-----
Chimpanzee	-----h-----
Monkey	-----h-----
House mouse	-----h-----
Chicken	-----h-----
Torafugu	e----r-a-----h-----
Zebrafish	e-----h-----
Fruit fly	-v-gqv-----s-hq-----

**FIGURE 6** Multiple amino acid sequence alignment of the peptide encoded by *WT1* of the patient with Human (*Homo sapiens*) (NCBI Reference Sequence: NM\_024424.5), Chimpanzee (*Pan troglodytes*) (NCBI Reference Sequence: XM\_016920639.2), Rhesus monkey (*Macaca mulatta*) (NCBI Reference Sequence: XM\_028833535.1), House mouse (*Mus musculus*) (NCBI Reference Sequence: NM\_144783.2), Chicken (*Gallus gallus*) (NCBI Reference Sequence: XM\_015286134.2), Torafugu (*Takifugu rubripes*) (NCBI Reference Sequence: XM\_011619095.2), Zebrafish (*Danio rerio*) (NCBI Reference Sequence: NM\_131046.2), and Fruit fly (*Drosophila melanogaster*) (NCBI Reference Sequence: NM\_001274762.1). Symbol (-) represents the amino acids identical to those of the patient

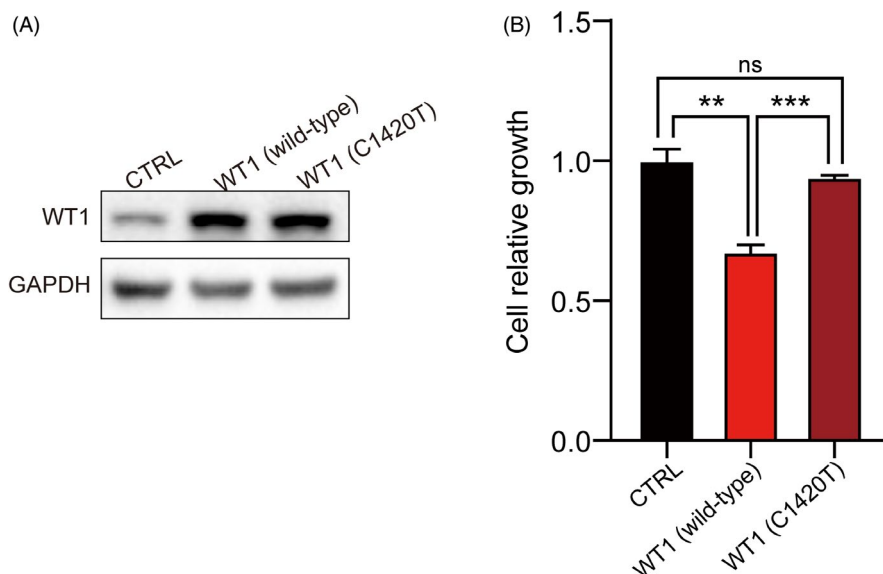
### 3.4 | Functional assays of the novel variant

In the cell growth inhibition assay, we found that G401 cells with pcDNA3.1-*WT1* (C1420 T) grew faster than those with pcDNA3.1-*WT1* (wild type) but slower than the control group. Significant differences were observed between the groups (Figure 7). The result indicates that the mutant variant of *WT1* (c.1420C>T, p. His474 Tyr) cannot function as well as the wild-type *WT1* as a tumor suppressor gene.

## 4 | DISCUSSION

We present a case of a patient with Wilms tumor, nephropathy, hermaphroditism, and a novel mutation in the *WT1* gene. All the pathological features that this patient had met the typical characteristics were described in the cases of Denys-Drash syndrome.<sup>17,18</sup>

**FIGURE 7** The function of WT1 (wild type and mutant variant) in G401 cells. A, The expression level of pcDNA3.1-WT1 (wild type) and pcDNA3.1-WT1 (C1420 T) was examined in a western blot analysis. B, Cell relative growth analysis. 3000 cells from each group were seeded in 96-well plate per well and cultured for 7 days. Thereafter, we detected the cell relative growth rate by the MTS assay. All data are presented as the mean  $\pm$  standard deviation from three independent experiments. Non-paired t-test was performed between the groups (\*\* $p < 0.05$ , \*\*\* $p < 0.005$ , ns: non-significance)



The human *WT1* gene is approximately 50 kb in length, spanning 10 exons.<sup>19,20</sup> The protein has four C2H2 zinc fingers (ZFs) for nucleic acid binding in the C-terminal,<sup>21,22</sup> while its NH2 terminus contains both transcriptional repression and activation domains. It is a transcription factor with diverse functions in cells, ranging from organogenesis to tumor suppression.<sup>23</sup> For this patient, we found a missense mutation in exon 9 (c.1420C>T, p. His474 Tyr) of the *WT1* gene that encodes ZF3. To the best of our knowledge, this is the first time this mutation is being reported in the literature.

In DDS, mutations in the ZF region can abolish the DNA-binding capacity and lead to sex ambiguity because of dysgenetic testis, diffuse mesangial sclerosis with chronic renal disease, and a high incidence of Wilms tumor.<sup>24</sup> In this study, we found that the histidine in *WT1* was a conserved residue and that the mutant variant could not function well as a tumor suppression gene. In addition, the Mutation Taster tool also suggests that it is a “disease-causing” mutant variant.

Mutant *WT1* disrupts the development and differentiation of podocytes. The c.1420C>T mutation in exon 9 induces an amino acid change from histidine to tyrosine in ZF3. Histidine is an important component of the zinc-finger structure. The binding affinity of the mutant peptides to the DNA target may become weaker. Studies have shown that *WT1* activates the transcription of the podocalyxin gene.<sup>25,26</sup> The *WT1* variant with a mutation in ZF9 may disrupt podocyte development and differentiation, leading to renal insufficiency. In mice with *WT1* knockout in podocytes, the podocyte foot processes disappeared and, consequently, glomerulosclerosis and proteinuria developed in mice. The results confirmed the essential role of *WT1* in podocyte maturation and maintenance.<sup>27-29</sup> In addition, a study of histological specimens from children with DDS found that *WT1* expression in podocytes was abnormal in 80% of patients.<sup>30</sup> For this patient, the mutation may play a crucial role in the process of nephrotic syndrome. Fortunately, the nephrotic syndrome was well controlled at the end of the follow-up period. We will continue to monitor the development of nephropathy in the child closely.

In addition, *WT1* also plays a key role in the regulation of *SRY* expression and sex determination. *WT1* and steroidogenic factor 1 (SF-1) are expressed in the urogenital ridge, which develops into the kidneys and gonads.<sup>31</sup> *WT1* associates with SF-1 and achieves a synergistic effect. The upregulation of the *SRY* gene and the promotion of Müllerian inhibiting substance (MIS) both rely on the synergism of *WT1* and SF-1 expressed in the bipotential gonad.<sup>32-34</sup> The mutant *WT1* may disrupt the synergy between *WT1* and SF-1, which leads to gonadal abnormalities in 46,XY individuals.<sup>35,36</sup> This may explain the correlation between gonadal abnormalities and mutations in the *WT1* gene in this patient.

## 5 | CONCLUSION

We report a novel mutation in *WT1* associated with DDS in a child. The uncommon missense mutation (c.1420C>T, p. His474 Tyr) in the *WT1* gene may be a crucial marker in DDS. *WT1* sequencing should be considered early in children with sexual dysplasia, especially in patients with a 46,XY karyotype.

## ACKNOWLEDGEMENTS

We thank Dr. Zhongwei Gu and Minju Li for kindly providing clinical data and material. Dr. Minju Li gave us valuable advices, and Dr. Zhongwei Gu provided excellent technical assistance. In addition, we thank the parents of the patient for the support in the study. This study was supported by National Natural Foundation of China (81801939) and Health Commission of Zhejiang Province (2019KY093).

## CONFLICT OF INTERESTS

There is no conflict of interests.

## DATA AVAILABILITY STATEMENT

All data used for the analysis in this study are available in China National GeneBank DataBase (URL: <https://db.cngb.org/cnsa/>, Accession Number: CNP0001670).

## ORCID

Faliang Wang  <https://orcid.org/0000-0002-8603-736X>

## REFERENCES

- Pelletier J, Bruening W, Kashtan CE, et al. Germline mutations in the Wilms' tumor suppressor gene are associated with abnormal urogenital development in Denys-Drash syndrome. *Cell*. 1991;67(2):437-447.
- Guaragna MS, Ribeiro de Andrade JG, de Freitas Carli B, Belangero VM, Maciel-Guerra AT, Guerra-Junior G, de Mello MP: WT1 haploinsufficiency supports milder renal manifestation in two patients with Denys-Drash syndrome. *Sexual development : genetics, molecular biology, evolution, endocrinology, embryology, and pathology of sex determination and differentiation*. 2017;11(1):34-39.
- Sugiyama H. WT1 (Wilms' tumor gene 1): biology and cancer immunotherapy. *Jpn J Clin Oncol*. 2010;40(5):377-387.
- Moore AW, McInnes L, Kreidberg J, Hastie ND, Schedl A. YAC complementation shows a requirement for Wt1 in the development of epicardium, adrenal gland and throughout nephrogenesis. *Development*. 1999;126(9):1845-1857.
- Discenza MT, Pelletier J. Insights into the physiological role of WT1 from studies of genetically modified mice. *Physiol Genomics*. 2004;16(3):287-300.
- Miller-Hodges E. Clinical aspects of WT1 and the kidney. *Methods Mol Biol*. 2016;1467:15-21.
- Royer-Pokora B, Beier M, Henzler M, et al. Twenty-four new cases of WT1 germline mutations and review of the literature: genotype/phenotype correlations for Wilms tumor development. *Am J Med Genet A*. 2004;127A(3):249-257.
- Wei X, Ju X, Yi X, et al. Identification of sequence variants in genetic disease-causing genes using targeted next-generation sequencing. *PLoS One*. 2011;6(12):e29500.
- Li H, Durbin R. Fast and accurate short read alignment with Burrows-Wheeler transform. *Bioinformatics*. 2009;25(14):1754-1760.
- Li R, Li Y, Fang X, et al. SNP detection for massively parallel whole-genome resequencing. *Genome Res*. 2009;19(6):1124-1132.
- Li H, Handsaker B, Wysoker A, et al. The Sequence Alignment/Map format and SAMtools. *Bioinformatics*. 2009;25(16):2078-2079.
- Dai Y, Liang S, Dong X, et al. Whole exome sequencing identified a novel DAG1 mutation in a patient with rare, mild and late age of onset muscular dystrophy-dystroglycanopathy. *J Cell Mol Med*. 2019;23(2):811-818.
- Richards S, Aziz N, Bale S, et al. Standards and guidelines for the interpretation of sequence variants: a joint consensus recommendation of the American College of Medical Genetics and Genomics and the Association for Molecular Pathology. *Genet Med*. 2015;17(5):405-424.
- Schwarz JM, Cooper DN, Schuelke M, Seelow D. MutationTaster2: mutation prediction for the deep-sequencing age. *Nat Methods*. 2014;11(4):361-362.
- Zhang R, Chen S, Han P, et al. Whole exome sequencing identified a homozygous novel variant in CEP290 gene causes Meckel syndrome. *J Cell Mol Med*. 2020;24(2):1906-1916.
- Han P, Wei G, Cai K, et al. Identification and functional characterization of mutations in LPL gene causing severe hypertriglyceridaemia and acute pancreatitis. *J Cell Mol Med*. 2020;24(2):1286-1299.
- Drash A, Sherman F, Hartmann WH, Blizzard RM. A syndrome of pseudohermaphroditism, Wilms' tumor, hypertension, and degenerative renal disease. *J Pediatr*. 1970;76(4):585-593.
- Mueller RF. The Denys-Drash syndrome. *J Med Genet*. 1994;31(6):471-477.
- Call KM, Glaser T, Ito CY, et al. Isolation and characterization of a zinc finger polypeptide gene at the human chromosome 11 Wilms' tumor locus. *Cell*. 1990;60(3):509-520.
- Gessler M, Poustka A, Cavenee W, Neve RL, Orkin SH, Bruns GAJN. Homozygous deletion in Wilms tumours of a zinc-finger gene identified by chromosome jumping. *Nature*. 1990;343(6260):774-778.
- Rauscher FJ, Morris JF, Tournay OE, Cook DM, Curran T. Binding of the Wilms' tumor locus zinc finger protein to the EGR-1 consensus sequence. *Science*. 1990;250(4985):1259-1262.
- Chirgadze YN, Boshkova EA, Polozov RV, et al. The electrostatic role of the Zn-Cys2His2 complex in binding of operator DNA with transcription factors: mouse EGR-1 from the Cys2His2 family. *J Biomol Struct Dyn*. 2018;36(15):3902-3915.
- Shandilya J, Toska E, Richard DJ, Medler KF, Roberts SG. WT1 interacts with MAD2 and regulates mitotic checkpoint function. *Nat Commun*. 2014;5:4903.
- Wang XN, Li ZS, Ren YU, et al. The Wilms tumor gene, Wt1, is critical for mouse spermatogenesis via regulation of sertoli cell polarity and is associated with non-obstructive azoospermia in humans. *PLoS Genet*. 2013;9(8):e1003645.
- Palmer RE, Kotsianti A, Cadman B, Boyd T, Gerald W, Haber DA. WT1 regulates the expression of the major glomerular podocyte membrane protein Podocalyxin. *Current biology : CB*. 2001;11(22):1805-1809.
- Dong L, Pietsch S, Tan Z, et al. Integration of cistronic and transcriptomic analyses identifies Nphs2, Mafk, and Magi2 as Wilms' tumor 1 target genes in podocyte differentiation and maintenance. *Journal of the American Society of Nephrology : JASN*. 2015;26(9):2118-2128.
- Gebeshuber CA, Kornauth C, Dong L, et al. Focal segmental glomerulosclerosis is induced by microRNA-193a and its downregulation of WT1. *Nat Med*. 2013;19(4):481-487.
- Chau Y-Y, Brownstein D, Mjoseng H, et al. Acute multiple organ failure in adult mice deleted for the developmental regulator Wt1. *PLoS Genet*. 2011;7(12):e1002404.
- Asfahani RI, Tahoun MM, Miller-Hodges EV, et al. Activation of podocyte Notch mediates early Wt1 glomerulopathy. *Kidney Int*. 2018;93(4):903-920.
- Yang Y, Jeanpierre C, Dressler GR, Lacoste M, Niaudet P, Gubler M-C. Gubler M-CJTAjop: WT1 and PAX-2 podocyte expression in Denys-Drash syndrome and isolated diffuse mesangial sclerosis. *Am J pathol*. 1999;154(1):181-192.
- Kim J, Prawitt D, Bardeesy N, et al. The Wilms' tumor suppressor gene (wt1) product regulates Dax-1 gene expression during gonadal differentiation. *Mol Cell Biol*. 1999;19(3):2289-2299.
- Mendonca BB, Domenice S, Arnhold IJP, Costa EMF. 46, XY disorders of sex development (DSD). *Clin Endocrinol (Oxf)*. 2009;70(2):173-187.
- Köhler B, Schumacher V, l'Allemand D, Royer-Pokora B, Grüters A. Germline Wilms tumor suppressor gene (WT1) mutation leading to isolated genital malformation without Wilms tumor or nephropathy. *J Pediatr*. 2001;138(3):421-424.
- Kalfa N, Gaspari L, Ollivier M, et al. Molecular genetics of hypospadias and cryptorchidism recent developments. *Clin Genet*. 2019;95(1):122-131.
- Kucinkas L, Just WJM. Human male sex determination and sexual differentiation: pathways, molecular interactions and genetic disorders. *Medicina (Kaunas)*. 2005;41(8):633-640.
- Biason-Lauber A. The battle of the sexes: human sex development and its disorders. *Results Probl Cell Differ*. 2016;58:337-382.

**How to cite this article:** Wang F, Cai J, Wang J, et al. A novel WT1 gene mutation in a chinese girl with denys-drash syndrome. *J Clin Lab Anal*. 2021;35:e23769. <https://doi.org/10.1002/jcla.23769>